



Biosorption of Acid Yellow 12 from simulated wastewater by non-viable *T. harzianum*: kinetics, isotherm and thermodynamic studies

V. Karthik¹ · K. Saravanan² · C. Patra³ · B. Ushadevi⁴ · S. Vairam⁴ · N. Selvaraju³

Received: 22 July 2018 / Revised: 25 September 2018 / Accepted: 15 October 2018 / Published online: 22 October 2018
© Islamic Azad University (IAU) 2018

Abstract

The current study deals with the biosorption of Acid Yellow 12 (AY 12) dye using dead fungal biomass *Trichoderma harzianum*. The dead fungal biomass was characterized using FTIR, XRD, TG–DTA and SEM–EDAX. Effect of various parameters on the efficiency of biosorption like pH, biosorbent dosage and temperature has also been analysed. The adsorption capacity was found to be higher at pH 4, with an initial dye concentration of 100 mg/L and biosorbent dosage of 0.4 g/L. The adsorption kinetics, isotherms and thermodynamic studies of dye adsorption onto the biomass were also investigated. The biosorption between the dye and biomass followed Freundlich adsorption isotherm. The biosorption followed pseudo-second-order kinetics. Negative value of ΔG° shows the spontaneous nature of biosorption process, and positive ΔH° reveals adsorption as an endothermic process. Since *T. harzianum* is a low-cost industrial by-product, it can be used as an effective novel biosorbent for the removal of textile dyes. It also acts as one of the cheap sources of biosorbent for the removal of dye Acid Yellow 12.

Keywords Biosorption · Acid Yellow 12 dye · *T. harzianum* · Adsorption kinetics · Adsorption isotherm

Introduction

Dyes play a vital role in textile, printing, plastics, food, cosmetic and pharmaceutical industries (Maurya et al. 2006; Mittal et al. 2010; Gupta et al. 2011; Saleh and Gupta 2012a, 2014; Saravanan et al. 2013a). It imparts colour to various commercial products. Over the years, the use of dyes has increased, and as a result of it, pollution level has also increased (Fomina and Gadd 2014; Gupta et al. 2013; Saravanan et al. 2013b; Ghaedi et al. 2015). Effluents discharged

from the above industries possess visible colours, and thus, when discharged to the water bodies without prior treatment, they tend to change the colour of the water bodies which can cause aesthetic problem. Apart from this, coloured water retards sunlight penetration which in turn directly affects the photosynthesis of the aquatic vegetation (Tan et al. 2010; Mohammadi et al. 2011; Saravanan et al. 2013c; Zhou et al. 2015).

Textile wastewaters are considered to be the most polluted water because of the presence of high amount of dyes. Discharging these effluents directly on land or water bodies adversely affects the ecosystem and makes the water unfit for drinking purpose because of the colourization of water (Pearce 2003; Saravanan et al. 2013d; Gupta et al. 2014; Robati et al. 2016). Physico-chemical methods are thus used to remove the colour from wastewater such as adsorption, precipitation, photo-oxidation, coagulation, flocculation, reduction, electrochemical treatment and photo-degradation (Maurya et al. 2006; Ahmaruzzaman and Gupta 2011; Karthikeyan et al. 2009; Khani et al. 2010; Gupta et al. 2013; Saravanan et al. 2015a).

Recently, microbial biomass has been used for the removal of contaminating dyes from the wastewater

Editorial responsibility: Shahid Hussain.

✉ N. Selvaraju
selva@iitg.ac.in

¹ Department of Industrial Biotechnology, Government College of Technology, Coimbatore 641013, India

² Department of Chemical Engineering, Kongu Engineering College, Perundurai, Erode 638060, India

³ Department of Biosciences and Bioengineering, Indian Institute of Technology, Guwahati, Assam 781039, India

⁴ Department of Chemistry, Government College of Technology, Coimbatore 641013, India



(Table 1). It has gained importance because using microbes is an eco-friendly and cost-effective process (Crini 2006; Gupta et al. 2015). Agreeable dismissal pursuance, extensibility, less contribution in terms of basic amount, detachment to toxic pollutants, ease of design, effortless operation are the major advantages of biosorption system for the control of water pollution (Hu 1996; Saleh and Gupta 2011, 2012b; Saravanan et al. 2015b; Rajendran et al. 2016). Microorganisms remove dyes from wastewater through any of the methods involving biosorption, bioaccumulation and biodegradation (Gao et al. 2010; Saravanan et al. 2013e; Devaraj et al. 2016).

Fungal biomass due to its sorbate scale availability, ability to grow in any expensive medium and easy harvesting procedures holds a clear-cut advantage over other microorganisms with respect to industrial exploitation, eco-friendly nature and it's easy process for remediation. Fungal species like *A. niger*, *A. wentii*, *A. foetidus* and *T. harzianum* are most widely used species for dye removal (Sivasamy and Sundarabai 2011).

The advantages of *T. harzianum* such as easy availability, cheaper cost, good mechanical properties and chemical stability in both alkaline and acidic conditions make them useful adsorbent in the biosorption studies. Besides, the dried fungi have a tough texture and have other physical characteristics. Dead fungal biomass is preferred for wastewater treatment because it is not affected by toxic wastes and chemicals and does not pollute the environment by releasing toxins and propagules (Fomina and Gadd 2014; Karthikeyan et al. 2012). To the best of our knowledge, there is no current report available on the use of *T. harzianum* for the removal of AY 12.

The present work reports on the study of the removal of AY 12 dye from wastewater by using the potential novel biosorbent, *T. harzianum*, via biosorption. Further, batch biosorption characteristics have also been determined by kinetic and equilibrium studies.

Materials and methods

Biosorbent cultivation and preparation

The *T. harzianum* was obtained from the MTCC, Chandigarh, and it was cultivated using the Sabouraud Dextrose Broth medium which is composed of peptone, dextrose and distilled water, maintained at pH 5.6. It was incubated for 7 days at 28 °C in a shaker. Dead biomass was obtained after 7 days by autoclaving at 121 °C for 15 min. Subsequently, the biomass was dried at 50 °C for 24 h and powdered in a mortar and pestle and used as such.

Preparation of dye solution

The Acid Yellow 12 (AY 12) (C₁₇H₁₅N₄NaO₄S, CAS no: 6359-84-8, C.I.18830, molecular weight: 394.38) was procured from Sigma-Aldrich and used without any further purification. A stock solution of AY 12 of 1000 ppm was prepared by using distilled water as a solvent and stored.

Characterization of biosorbent

The nature of functional groups in non-viable *T. harzianum* was found by FTIR Spectrophotometer (Burke Optik GmbH, TENSOR 27, Germany). The surface morphology of biomass before and after biosorption was analysed using SEM images recorded using Hitachi (Japan) S-3000H. Thermal stability of the biosorbent was analysed by a Thermogravimetric Analyzer (SQT Q600).

Biosorption experiments

All the biosorption experiments were carried out using variable amounts of dead fungal biomass from 0.1 to 0.5 g in 100-mL portions of dye solutions of concentrations varying from 50 to 350 mg/L, subjected to shaking the solutions at 120 rpm for 4 h in a rotary shaker. The interaction was followed by centrifugation at 10,000 rpm for 10 min.

Table 1 Comparison of various biosorbent capacities for the removal of acid yellow

Adsorbent	Adsorbate	Adsorption capacity (mg/g)	References
<i>E. coli</i>	Reactive yellow 2	52.4	Hu (1996)
Daedaleaflavida	Reactive yellow	11.11	Chander and Arora (2007)
Hydroxyapatite	Reactive yellow 84	52.25	Barka et al. (2011)
(Co, Ni) ₃ O ₄ /Al ₂ O ₃	Reactive yellow	18.78	Mohammad et al. (2016)
Chitin	MY 5	39	McKay et al. (1982)
Zeolite	RY 176	12.5	Faki et al. (2008)
Peanut husk	IndosolYellow	25.9	Sadaf and Bhatti (2014)
<i>T. harzianum</i>	Acid Yellow	78.39	Present study



Supernatants were carefully collected, and the amount of AY 12 remained in the supernatant was determined by measuring absorbance measurements at 428 nm using UV–Visible spectrophotometer.

The per cent removal of dye from various aqueous solutions was determined in the equation

$$\% \text{ dye removal} = (C_o - C_e) / C_o \times 100 \quad (1)$$

Adsorption of AY 12 on *T. harzianum* was measured at pH 1–12, by adjusting the pH of the experimental solutions using HCl or NaOH (1 N). The optimum pH was determined from the plot drawn with pH against % dye removal at 20, 30, 37 and 45 °C, and the effect of temperature on adsorption was also studied. The data collected are summarized in Table 1.

Isotherm model studies

The equilibrium data were used to study various isotherm models, viz. Langmuir, Freundlich, Temkin and Dubinin–Radushkevich isotherm models, to understand the proper interaction between AY 12 and *T. harzianum*.

Adsorption kinetics

The kinetic measurements were carried out by adopting similar procedure as explained before at pH 4, and adsorption was measured at different time intervals varying from 10 to 120 min. The data collected are summarized in Table 3.

Thermodynamic studies

Thermodynamic parameters like change in Gibbs free energy (ΔG°), change in enthalpy (ΔH°) and change in entropy (ΔS°) were calculated using the equilibrium data at different temperatures.

Results and discussion

Characterization of biosorbent

FTIR

The FTIR spectra of the biomass and dye-loaded biomass are shown in Fig. 1a. The intense band around 3400 cm^{-1} is due to the stretching frequency of –OH groups of the polysaccharides and proteins present in the biomass sample. The sharp bands around 2900 cm^{-1} , 1640 cm^{-1} , 1440 cm^{-1} , 1250 cm^{-1} and 1025 cm^{-1} are due to –C–H stretching, –C=C– stretch of alkene, –CH₂ bending, –C–O–C– (aliphatic ether) bending and –C=O stretching of COOH frequencies, respectively. The IR spectrum of dye-loaded biomass has all the bands corresponding to biomass. Further, it shows a more intense and broadband around 3400 cm^{-1} due to the presence of adsorbed water and in addition depicts the presence of the –N=N stretching frequency at 1548 cm^{-1} .

XRD

The XRD pattern of biosorbent exhibited a semi-crystalline peak at $2\theta = 21.38^\circ$ and 39.42° shown in Fig. 1b. These polysaccharides are found semi-crystalline in nature where disarray in the alignment of network chains is found sparingly. The semi-crystalline nature of the polymeric chains gives an advantage in adsorption where the crystal arrangement can provide a space for accommodating particles of different structure and shape (Njoku et al. 2014). This attributes the adsorbing ability of the biosorbent with their structural components. Further, it is understood that there is no defect in the crystal pattern (Fomina and Gadd 2014). This defect less pattern shows the purity of the biosorbent with no other contaminants on the biomass after cultivation which directly can be used for adsorption of various contaminants. With

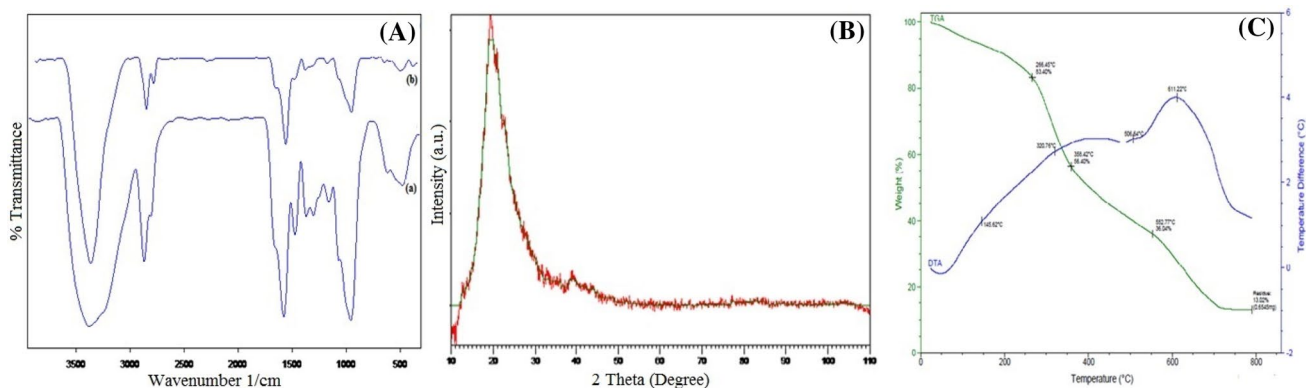


Fig. 1 a FTIR spectra before and after dye adsorption; b XRD spectra; c thermogravimetric analysis of dead fungal biomass *T. harzianum*



uniform semi-crystal planes, the structure of the biosorbent is highly stable and organized into a definite construct that can withstand even extreme varying condition like pH and temperature, thereby enabling it to be used as a biosorbent at extreme ambience where biosorption is required. The XRD studies have revealed the semi-crystal nature of the biosorbent and presence of chitin-like crystal patterns that are coherent with the previous analysis.

TG–DTA

The TG–DTA thermogram recorded in an inert nitrogen atmosphere with the temperature range of 30°–800 °C of the dead fungal biomass is shown in Fig. 1c. The plateau near 200 °C can be attributed to dehydration of moisture present in the fungal biomass. Between temperatures, 200° to 550 °C, major degradation (~60%) occurs, where combustion of the biopolymers (such as proteins and polysaccharides, chitin, etc.) takes place. During the first two stages, the most reactive substances are affected, whereas the other remaining substances are decomposed after 550 °C. The biomass shows a continuous decomposition, showing the endotherm at 100 °C due to dehydration and exotherm at 380 °C (broad) and 610 °C (medium sharp) due to oxidative decomposition of biomass, which results in a residue to almost 13%.

SEM–EDAX

Size and shape of the biosorbent are the invigorating characteristic feature that can significantly influence the adsorbing capacity of the biosorbent. Moreover, the surface texture of the biosorbent would be varied with effect to the adsorption and their allied effects. Uniform distribution is a cardinal criterion for the proper biosorption of contaminants on the entire surface area of the biosorbent. The uniform distribution can be ascribed from porosity, roughness and structure of the biosorbent. These distributions can be understood from analysing the biomass using electron microscopes. The SEM image divulges the difference in their surface structure of native biosorbent. With this regard, this study focused on examining the morphological properties of the biosorbent in concern with adsorption and related changes.

The SEM images of the biosorbent are shown in Fig. 2a–c. The fungal biomass was found with stable tubular structures with small coils and short branches. These short coil and branches are young hyphae with growing colony edge, increasing the incidence of curling tips. The dense and structured hyphae show the viability of the organism with uniform integrity on the surface of the hyphae. Moreover, the growth is seen appressed and no other colonization is observed in the hyphae showing that as a pure culture (Fomina and Gadd 2014). There is a uniform mat-like

knitted structure that is due to the presence of structural polymer chitin which provides this integrity and stable structure that is in agreement with the FTIR functional group that correspond to chitin. In all the SEM images, a rough surface without porosity is observed that conceivably might be related to their high molecular packing, with inter- or intramolecular hydrogen bonds. This is a characteristic feature of chitin that possesses similar high crystalline nature (Puchana-Rosero et al. 2017). The overall morphology of the biosorbent is found to be with turgor nature that would make advantageous for dye or contaminant removal at even adverse condition without any compromise in the functionality, and future studies could lead into reuse of the biosorbent with appropriate research.

X-ray micro-analysis in conjunction with scanning electron was carried out to determine the elemental composition of the biosorbent (Fig. 2d). EDAX outcome shows a typical elemental composition that includes carbon, nitrogen and oxygen which are integral components of the hyphae being an organic material. Moreover, the spectrum shows the presence of calcium, silica and phosphorous also. The presence of potassium and calcium would have been from the biosorbent medium where mycelia were grown. Phosphorous presence can also be attributed to organic nature of the sorbent (Fomina and Gadd 2014). The intrigue traces of these elements are inert and thus have been seen in the EDAX apart from the typical composition of organic compounds (Hu 1996). Similarly, the presence of C, H, O and N is found in the elemental analysis reported earlier for chitin (Sivasamy and Sundarabal 2011). Since fungal hyphae contain chitin as a significant component in their cell wall, similar elemental composition of spectra was seen in the biosorbent EDAX spectra. The overall spectral information is in agreement with FTIR and TG–DTA interpretations. The biosorbent nature is much of analogous to chitin the second largest available polymer in the planet. These results lead to new insights into fungal biomass-based biosorption for various contaminants removal such as dye, metal and hazardous chemicals.

Adsorption studies

Effect of biosorbent dosage

Parameters like the initial concentration, pH of solution and temperature were kept constant, and the biosorbent dosage was varied to study its effect on biosorption of AY 12 dye onto dead fungal biomass of *T. harzianum*. Figure 3 shows that percentage removal of the dye heightened with increasing biosorbent dose. The removal percentage started from 55% and reached to a maximum of 93% with regard to the biosorbent dosage level. These results prove the fact that biosorbent dosage level will influence

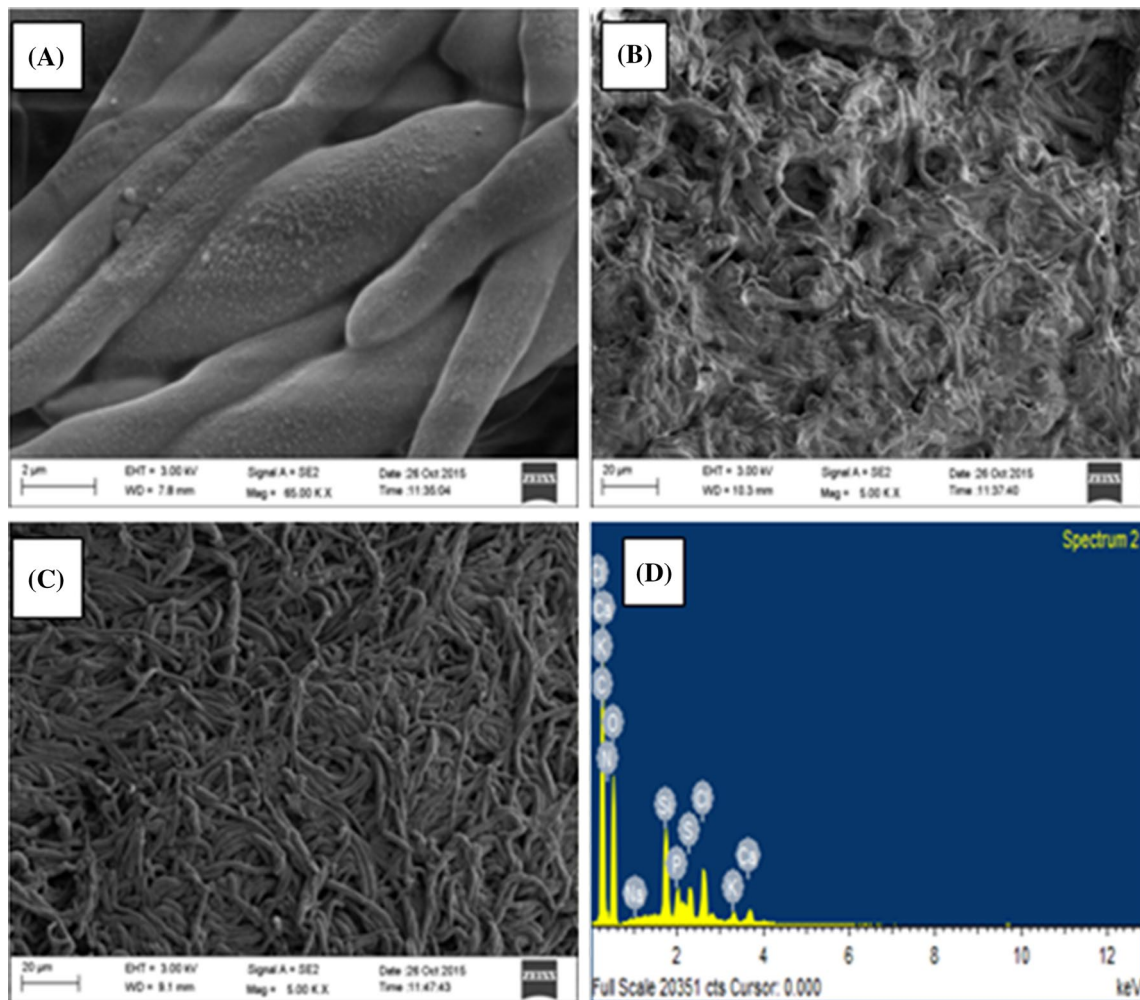


Fig. 2 a–c SEM images of dead fungal biomass *T. harzianum*; d EDAX of fungal biomass after biosorption of dye

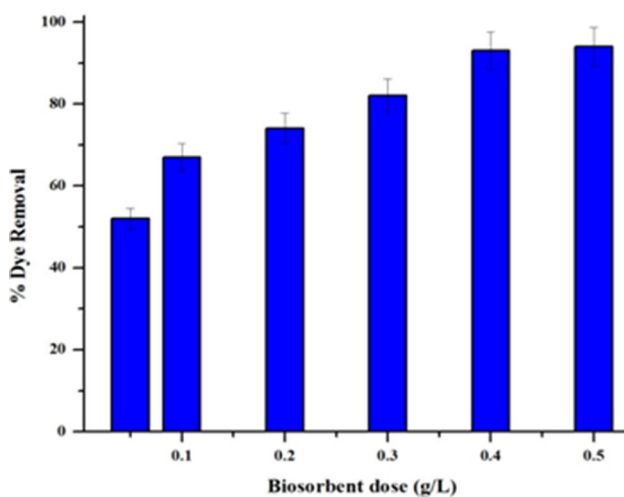


Fig. 3 Percentage removal of the dye adsorbed with increasing biosorbent dose by dead fungal biomass of *T. harzianum*

the dye removal ability. The results show that gradual and consistent removal ability increased with increasing dosage levels from 0.1 to 0.5 g/L. The greater dosage provides a larger number of adsorbing sites which facilitates increased biosorption. Therefore, percentage removal increases with increasing biosorbent dose and vice versa. The results were in coherence with *F. fomentarius* and *P. igniarius* (Maurya et al. 2006) and peanut husk (Sadaf and Bhatti 2014). The biosorbent dosage has a huge impact on the ability of dead fungal biomass ability to adsorb AY 12.

Effect of pH

The effect of pH on dye removal was studied under identical conditions for AY 12. In this study, the maximum dye removal was seen in pH 4 with 91% adsorption efficiency. These results are shown in Fig. 4. The results exhibit the influence of pH on the dye removal by dead fungal biomass as a biosorbent. The dye removal percentage was seen

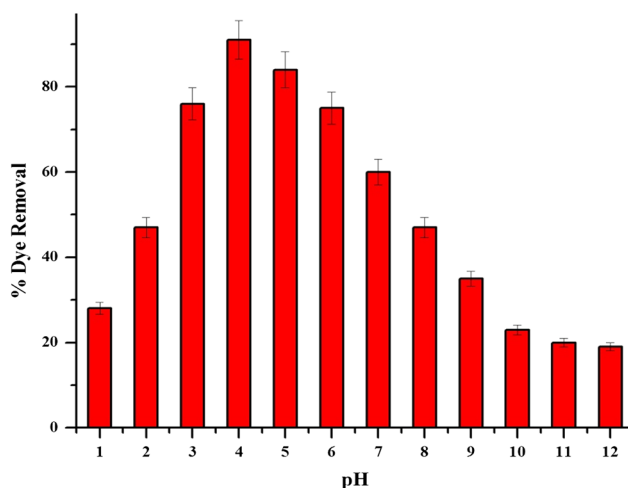


Fig. 4 Percentage removal of the dye adsorbed with increasing pH by dead fungal biomass of *T. harzianum*

progressively elevated at acidic pH and reached a maximum at pH 4 which then was seen to deteriorate. Thus, at pH below 4, excess protonation tends to neutralize the anionic surfaces of the biosorbents and the anionic dye causing low adsorption among them. These effects of pH in biosorption efficacy of the dead fungal biomass attributed to its functionality and effects on dye removal. Moreover, after the maximum dye removal at pH 4, there is a significant reduction in the biosorption capacity of the dead fungal mass in alkaline pH due to the excessive hydroxyl ions. The hydroxyl

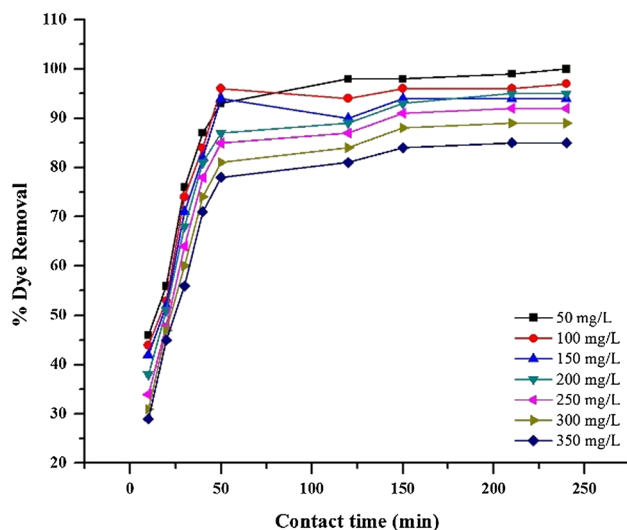


Fig. 5 Percentage removal of dye with time as a function by dead fungal biomass of *T. harzianum*

ion strives to occupy the binding sites of the dye against the anion of dye that actually binds. This is the major reason where the biosorbent after its optimal pH slowly loses its efficacy for biosorption. Connatural effects were observed in natural sorbents like chitosan (Iqbal et al. 2011).

Table 2 Biosorption isotherm parameters and correlation coefficient for AY 12 with *T. harzianum* inactivated biomass at various temperatures

Parameter	Temperature (°C)			
	25 °C	30 °C	35 °C	40 °C
<i>Langmuir model</i>				
q_0 (mg/g)	63.16	69.76	72.43	78.39
b_L (L/mg)	0.0048	0.0053	0.0055	0.0061
R^2	0.909	0.923	0.912	0.916
<i>Freundlich model</i>				
n	1.599	1.570	1.496	1.620
k_f ($\text{mg}^{1-1/n}\text{L}^{1/n}\text{g}^{-1}$)	8.29	8.59	9.77	12.27
R^2	0.982	0.987	0.993	0.986
<i>Temkin model</i>				
b_T (J/mg)	31.03	34.93	36.445	39.05
a_T (L/g)	2.602	2.555	2.924	2.459
R^2	0.853	0.881	0.821	0.891
<i>Dubinin–Raduskevich model</i>				
q_D (mg/g)	0.947	1.026	1.201	1.140
β (mol^2/J^2)	3.55	3.36	3.64	3.56
E (kJ/mol)	8.375	9.385	9.370	9.774
R^2	0.814	0.822	0.832	0.893



Effect of the initial dye concentration and contact time

An initial concentration of 100 mg/L of AY 12 dye was used to study the percentage removal with time as a function by dead fungal biomass of *T. harzianum* (Fig. 5). Uptake of dye by dead fungal biomass occurs at a rapid rate, corresponding to 91.87% removal at an equilibrium time of 150 min. At this initial stage, the rate of biosorption was to a greater extent which later went depreciating that possibly might be due to the availability of entire active bare surface. The progress of the dye removal percentage after a contact time of 150 min was relatively not significant, and hence, it was fixed as the optimum contact time (Garg 2004). Moreover, the dye removal percentage was elevated at the beginning due to the accessible surface that was much available for the dye to be adsorbed. These findings exhibit the surface area of the biosorbent with respect to the time of contact with dye has influence in dye removal activity (Chiou and Chuang 2006).

Biosorption isotherm

Biosorption isotherm parameters and correlation coefficient for AY 12 with *T. harzianum* inactivated biomass at various temperatures are given in Table 2. The Langmuir adsorption capacity increases 63.16 to 78.39 mg/g while increasing the temperature from 25 to 40 °C. The correlation coefficient (R^2) ranges in between 0.909 and 0.923 for the range of temperature studied. The monolayer adsorption capacity calculated by Langmuir model shows that there is no sequential variation with respect to temperature. The Freundlich constant (k_f) increases from 8.29 to 12.27 $\text{mg}^{1-1/n} \text{L}^{1/n} \text{g}^{1/n}$ for a temperature rise from 25 to 40 °C. The Freundlich constant k_f has been utilized as a relative measure of biosorption capacity of the biosorbent. A high value of k_f shows easy uptake of the dye. The slope $1/n$ measures the surface heterogeneity. Heterogeneity becomes more prevalent as $1/n$ gets closer to zero. For $1/n = 1$, a partition between the two phases is independent of the concentration. Value for $1/n$ below 1 indicates a normal and favourable adsorption.

The Freundlich model represents the biosorption of AY 12 dyes is very well. In order to decide which type of isotherm fits the experimental data better, the applicability of the model was established from the R^2 value (Njoku et al. 2014). Langmuir model does not fit properly, and to explain the trait of adsorption with R^2 rather Freundlich model displays higher fit ($R^2 = 0.982$ to 0.993). The values of Temkin constants, sorption potential, a_T , and heat of sorption, b_T , obtained from the plot of q_e versus $\ln C_e$ are found to vary from 2.459 to 2.924 and 31.03 to 39.05. They increase linearly with increasing temperature of the solutions. This result is similar to the results reported by Gao et al. 2010 for Langmuir monolayer adsorption capacity.

The D–R model constant q_D (mg/g) is found to vary from the experimental data. The magnitude of E varies from 8.375 to 9.774 kJ/mol. These values indicate that the bonding between the dye and adsorbent is chemisorption. However, the large deviation of q_D (mg/g) from the experimental data and poor R^2 obtained for D–R plot R^2 (0.814–0.893) suggest that the activation energy calculated based on D–R plot may not be the actual one (Vargas et al. 2012).

Biosorption kinetics

Pseudo-first-order kinetic model

In order to describe the pseudo-first-order kinetic Model, the following equation was used (Zhang et al. 2014).

$$\log (q_e - q_t) = \log q_e - \frac{k_1}{2.303} t \quad (2)$$

Plots of “ $\log (q_e - q_t)$ ” versus “ t ” at various temperatures are shown in Fig. 6a. In addition, the $q_{e(\text{exp})}$ values do not concur considerably with the computed $q_{e(\text{cal})}$ values at different temperatures (0.860–0.892) and also the R^2 values are relatively down. The k_1 values for different temperatures (0.0314–0.0437) are influential. The biosorption kinetic data for the various temperatures studied show a deviation of the straight line. Thus, the biosorption of AY 12 onto fungal biomass does not fit the first-order kinetic model.

Pseudo-second-order kinetic model

The pseudo-second-order kinetic model is represented by Eq. (3) (Zhang et al. 2014)

$$\frac{t}{q_t} = \frac{1}{k_2 q_e^2} + \frac{t}{q_e} \quad (3)$$

A plot of “ t/q_t ” versus “ t ” at several initial dye concentrations and temperatures is shown in Fig. 6b. The pseudo-second-order rate constant (k_2) gains initially and then decrements on increasing the temperature (25–40 °C). The pseudo-second-order rate constant (k_2) ranges from 2.0×10^{-4} to 1.9×10^{-4} g/mg/min for the different temperatures studied.

The figured equilibrium biosorption capability $q_{e(\text{cal})}$ is determined by pseudo-second-order model, and the results agree with quite well to that $q_{e(\text{exp})}$. The biosorption of AY 12 is better explained by pseudo-second-order kinetics as it shows very high for about $R^2 = 0.994 \sim 0.997$ (temperature). The application of the pseudo-second-order kinetic model indicates that the biosorption process of AY 12 onto is chemisorption and the rate-determining step is probably surface biosorption. These outcomes go along with the

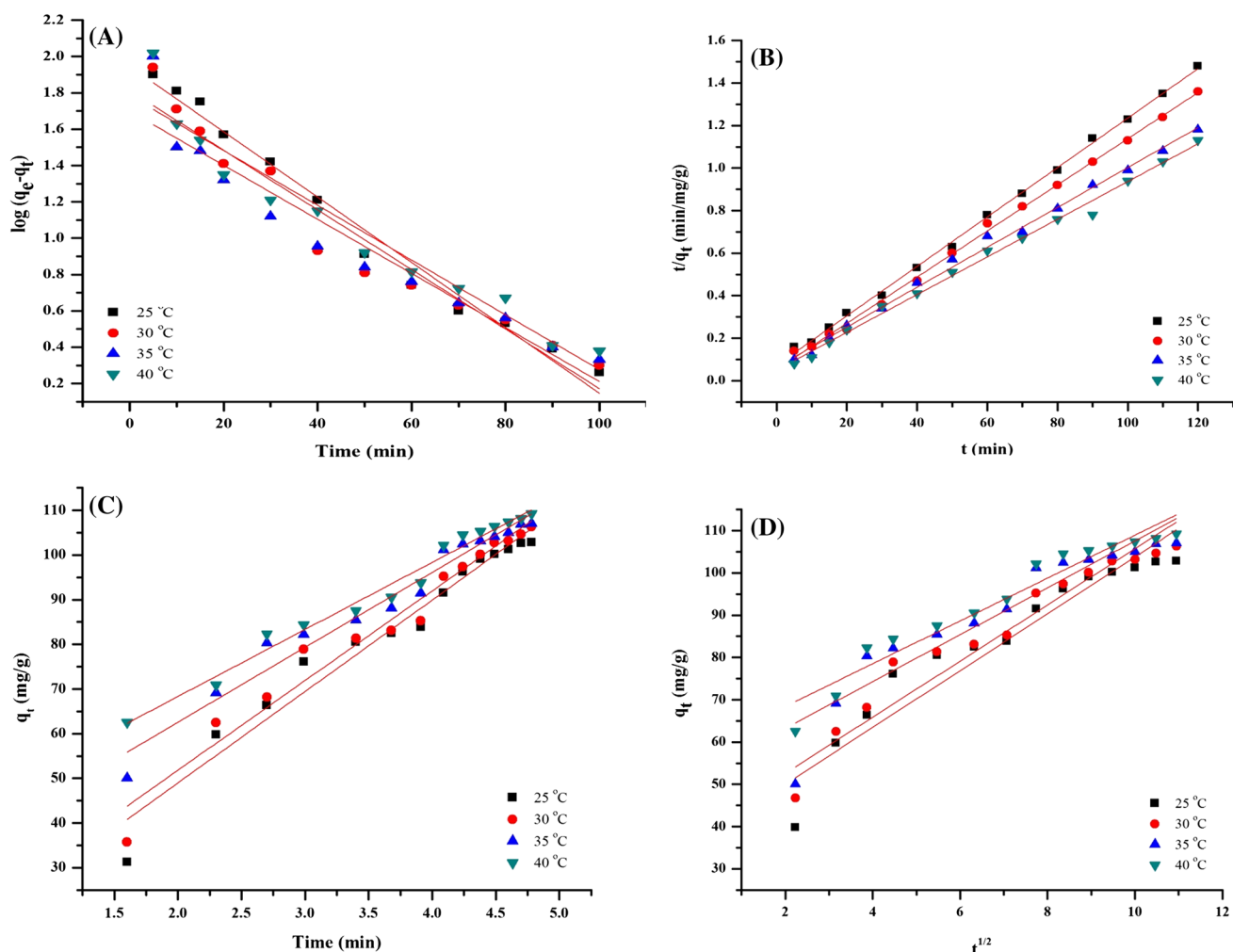


Fig. 6 a Plots of “ $\log (q_e - q_t)$ ” versus “ t ” at various temperatures. b Plot of “ t/q_t ” versus “ t ” at several initial dye concentrations and temperatures. c Plot of “ $\ln t$ ” versus “ q_t ” at various initial dye concentrations and temperatures. d Plot of “ q_t ” versus “ $t^{1/2}$ ”

reports of adsorption of Crystal Violet, Reactive Red-120 by *Lentinussajor-caju* (Bayramoglu and Yakup Arica 2007).

Elovich kinetic model

The adsorption equilibrium capacity of biosorbent for Elovich model is calculated by Eq. 4 and is given below.

$$q_e = \left(\frac{1}{\beta}\right) \ln(\alpha\beta) + \left(\frac{1}{\beta}\right) \ln t \quad (4)$$

A plot of “ $\ln t$ ” versus “ q_t ” at various initial dye concentrations and temperatures is shown in Fig. 6c. The initial sorption rate (α) increases from 6.032 to 7.135 mg/g/min with the increase in temperature from 25 to 40 °C. A similar course of the rapid initial uptake was found experimentally. On the other hand, the desorption coefficient (β) diminishes

with elevating temperature (24.93–22.86). On heightening the temperature, β increases initially and then decreases (Vargas et al. 2012).

Intraparticle diffusion model

The adsorption equilibrium capacity of biosorbent for intraparticle diffusion model is calculated by Eq. 5 and is given below

$$q_e = K_{id}t^{1/2} + C \quad (5)$$

The intraparticle diffusion model for the sorption of AY 12 at various initial dye concentrations and temperatures is given in Fig. 6d, respectively, and the results are given in Table 3. The plot of “ q_t ” versus “ $t^{1/2}$ ”, would yield a straight line passing through the origin if the biosorption process

Table 3 Effect of the initial dye concentration and temperature on biosorption kinetic parameters for AY 12 with *T. harzianum* inactivated biomass

Parameter	Temperature (°C)			
	25 °C	30 °C	35 °C	40 °C
<i>Pseudo-first-order kinetic model</i>				
$q_{e \text{ exp}}$ (mg/g)	81	88	101	106
k_1 (min^{-1})	0.0437	0.039	0.0368	0.0316
$q_{e \text{ cal}}$ (mg/g)	6.390	7.134	7.675	8.680
R^2	0.860	0.866	0.877	0.892
<i>Pseudo-second-order kinetic model</i>				
$k_2 \times 10^{-4}$ (g/mg/min)	2.0	2.8	1.5	1.9
$q_{e \text{ cal}}$ (mg/g)	80.64	89.28	100	105.2
R^2	0.997	0.997	0.994	0.994
<i>Elovich kinetic model</i>				
β (mg/g/min)	24.93	27.19	29.62	22.86
α (g/mg)	6.032	6.057	7.337	7.125
R^2	0.993	0.882	0.893	0.863
<i>Intraparticle diffusion model</i>				
k_{id} (mg/g/min ^{1/2})	9.107	9.249	9.931	10.941
R^2	0.859	0.884	0.832	0.889

Table 4 Calculated thermodynamic parameters for the biosorption of Acid Yellow 12 upon inactivated *T. harzianum* biomass at different temperatures

Temperature (K)	ΔG° (kJ/mol)	ΔH° (kJ/mol)	ΔS° (J/mol K)
298	−5.51	26.90	108.58
303	−6.05		
310	−6.81		
313	−7.14		

obeyed the intraparticle diffusion. The kinetic rate constant was obtained for different temperatures (9.107–10.941 mg/g/min^{1/2}).

The linear component of the plot for a wide range of contact time between biosorbent and sorbate would not move through the origin. This deflection from the origin or near the saturation region may be the result of the wavering mass transfer in the initial and final levels of biosorption. When the plots do not pass through the origin, this is declarative of some degree of boundary layer control. This subsequently designates that the intraparticle diffusion is not the only rate-limiting step, but also other kinetic models may control the rate of biosorption, entirely been operated simultaneously (Behnajady et al. 2007).

The beginning curved portions may be due to the boundary layer diffusion effect, while the terminal linear portions might be due to intraparticle diffusion effectuates. The biosorption data suggest that the removal of dye from aqueous phase was a rather composite

process, necessitating both boundary layer diffusion and intraparticle diffusion. The correlation coefficient R^2 (0.684–0.759) is accompanied by the intraparticle diffusion R^2 (0.730–0.977). The high correlation coefficient shows that pore diffusion acts as a major character for the biosorption of AY 12. Alike course was observed in equilibrium and kinetic studies on the removal of Congo Red dye with polyethyleneimine-modified wheat straw (Shang et al. 2016).

Thermodynamic study

The spontaneous biosorption process can be calculated from certain thermodynamic parameters (energy, entropy). The reversible process of AY 12 biosorption can be given by the following equation

$$\text{Dye in solution} = \text{dye} - \text{mixed biosorbent}$$



Calculation for Gibbs free energy can be determined by K_D (distribution constant)

$$K_D = \frac{q_e}{c_e} \quad (6)$$

$$\Delta G = -RT \ln K_D \quad (7)$$

$$\ln K_D = \frac{-\Delta G}{RT} = \frac{-\Delta H}{RT} + \frac{\Delta S}{R} \quad (8)$$

where $R = 8.314 \text{ J/mol k}$, $T =$ absolute temperature, the ΔS value can be obtained from the slope, whereas ΔH can be calculated (Table 4) from the van't Hoff plot ($\ln K_D$ vs. $1/T$).

The negative value of ΔG depicts that the biosorption is spontaneous, and the mixed biosorbent has higher affinity at a higher temperature. An increase in temperature and decrease in magnitude (ΔG) have the characteristics of reduction in the spontaneity degree. The change in standard enthalpy value of ΔH is 26.895 kJ/mol . The positive ΔH value depicts that the biosorption of AY 12 dye is an endothermic process and represents the affinity of mixed biosorbent for AY 12.

This concept could be elucidated by the availability of more active sites of adsorbent at higher temperature due to the increased surface activity and increased kinetic energy of AY 12 molecules. The positive ΔS value implies the randomness of the AY 12 biosorption. This evidences the good affinity of AY 12 towards the biosorbent and declared some structural changes in sorbate and biosorbent.

Conclusion

From the present work, it can be concluded that the non-viable biomass (used for study) is a cheap and an efficient adsorbent for AY 12 dye at pH 4, which, however, is normally maintained during dyeing conditions. The adsorption kinetics is found to follow the pseudo-second order and Freundlich isotherm. The biosorption process was spontaneous and endothermic, and also it is eco-friendly, economical and effective for the removal of wastewater.

Acknowledgements The authors wish to acknowledge Centre of Excellence/Environmental Science/TEQIP-Phase-II of Government College of Technology, Coimbatore, for the financial assistance. We would also like to thank the editor and all the reviewers for all their valuable suggestions and comments.

References

- Ahmaruzzaman M, Gupta VK (2011) Rice husk and its ash as low-cost adsorbents in water and wastewater treatment. *Ind Eng Chem Res* 50:13589–13613. <https://doi.org/10.1021/ie201477c>
- Barka N, Qourzal S, Assabbane A, Nounah A, Ait-Ichou Y (2011) Removal of Reactive Yellow 84 from aqueous solutions by adsorption onto hydroxyapatite. *J Saudi Chemical Soc* 15:263–267. <https://doi.org/10.1016/j.jscs.2010.10.002>
- Bayramoğlu G, Yakup Arica M (2007) Biosorption of benzidine based textile dyes “Direct Blue 1 and Direct Red 128” using native and heat-treated biomass of *Trametes versicolor*. *J Hazard Mater* 143:135–143. <https://doi.org/10.1016/j.jhazmat.2006.09.002>
- Behnajady MA, Modirshahla N, Daneshvar N, Rabbani M (2007) Photocatalytic degradation of an azo dye in a tubular continuous-flow photoreactor with immobilized TiO_2 on glass plates. *Chem Eng J* 127:167–176. <https://doi.org/10.1016/j.cej.2006.09.013>
- Chander M, Arora DS (2007) Evaluation of some white-rot fungi for their potential to decolourise industrial dyes. *Dyes Pigments* 72:192–198. <https://doi.org/10.1016/j.dyepig.2005.08.023>
- Chiou M-S, Chuang G-S (2006) Competitive adsorption of dye metanil yellow and RB15 in acid solutions on chemically cross-linked chitosan beads. *Chemosphere* 62:731–740. <https://doi.org/10.1016/j.chemosphere.2005.04.068>
- Crini G (2006) Non-conventional low-cost adsorbents for dye removal: a review. *Bioresour Technol* 97:1061–1085. <https://doi.org/10.1016/j.biortech.2005.05.001>
- Devaraj M, Saravanan R, Deivasigamani R, Gupta VK, Gracia F, Jayadevan S (2016) Fabrication of novel shape Cu and Cu/Cu₂O nanoparticles modified electrode for the determination of dopamine and paracetamol. *J Mol Liq* 221:930–941. <https://doi.org/10.1016/j.molliq.2016.06.028>
- Faki A, Turan M, Ozdemir O, Turan AZ (2008) Analysis of fixed-bed column adsorption of Reactive Yellow 176 onto surfactant-modified zeolite. *Ind Eng Chem Res* 47:6999–7004. <https://doi.org/10.1021/ie800097k>
- Fomina M, Gadd GM (2014) Biosorption: current perspectives on concept, definition and application. *Bioresour Technol* 160:3–14. <https://doi.org/10.1016/j.biortech.2013.12.102>
- Gao J, Zhang Q, Su K, Chen R, Peng Y (2010) Biosorption of Acid Yellow 17 from aqueous solution by non-living aerobic granular sludge. *J Hazard Mater* 174:215–225. <https://doi.org/10.1016/j.jhazmat.2009.09.039>
- Garg V (2004) Basic dye (methylene blue) removal from simulated wastewater by adsorption using Indian Rosewood sawdust: a timber industry waste. *Dyes Pigments* 63:243–250. <https://doi.org/10.1016/j.dyepig.2004.03.005>
- Ghaedi M, Hajjati S, Mahmudi Z, Tyagi I, Agarwal S, Maity A, Gupta VK (2015) Modeling of competitive ultrasonic assisted removal of the dyes—methylene blue and Safranin-O using Fe_3O_4 nanoparticles. *Chem Eng J* 268:28–37. <https://doi.org/10.1016/j.cej.2014.12.090>
- Gupta VK, Jain R, Nayak A, Agarwal S, Shrivastava M (2011) Removal of the hazardous dye—tartrazine by photodegradation on titanium dioxide surface. *Mater Sci Eng C* 31:1062–1067. <https://doi.org/10.1016/j.msec.2011.03.006>
- Gupta VK, Kumar R, Nayak A, Saleh TA, Barakat MA (2013) Adsorptive removal of dyes from aqueous solution onto carbon nanotubes: a review. *Adv Coll Interface Sci* 193–194:24–34. <https://doi.org/10.1016/j.cis.2013.03.003>
- Gupta VK, Nayak A, Agarwal S, Tyagi I (2014) Potential of activated carbon from waste rubber tire for the adsorption of



- phenolics: effect of pre-treatment conditions. *J Colloid Interface Sci* 417:420–430. <https://doi.org/10.1016/j.jcis.2013.11.067>
- Gupta VK, Nayak A, Agarwal S (2015) Bioadsorbents for remediation of heavy metals: current status and their future prospects. *Environ Eng Res* 20:1–18. <https://doi.org/10.4491/eeer.2015.018>
- Hu T-L (1996) Removal of reactive dyes from aqueous solution by different bacterial genera. *Water Sci Technol* 34:89–95. [https://doi.org/10.1016/S0273-1223\(96\)00701-9](https://doi.org/10.1016/S0273-1223(96)00701-9)
- Iqbal J, Wattoo FH, Wattoo MHS, Malik R, Tirmizi SA, Imran M, Ghangro AB (2011) Adsorption of acid yellow dye on flakes of chitosan prepared from fishery wastes. *Arab J Chem* 4:389–395. <https://doi.org/10.1016/j.arabjc.2010.07.007>
- Karthikeyan K, Kalpana D, Renganathan NG (2009) Synthesis and characterization of ZnCo₂O₄ nanomaterial for symmetric supercapacitor applications. *Ionics* 15:107–110. <https://doi.org/10.1007/s11581-008-0227-y>
- Karthikeyan S, Gupta VK, Boopathy R, Titus A, Sekaran G (2012) A new approach for the degradation of high concentration of aromatic amine by heterocatalytic Fenton oxidation: kinetic and spectroscopic studies. *J Mol Liq* 173:153–163. <https://doi.org/10.1016/j.molliq.2012.06.022>
- Khani H, Rofouei MK, Arab P, Gupta VK, Vafaei Z (2010) Multi-walled carbon nanotubes-ionic liquid-carbon paste electrode as a super selectivity sensor: application to potentiometric monitoring of mercury ion(II). *J Hazard Mater* 183:402–409. <https://doi.org/10.1016/j.jhazmat.2010.07.039>
- Maurya NS, Mittal AK, Cornet P, Rother E (2006) Biosorption of dyes using dead macro fungi: effect of dye structure, ionic strength and pH. *Bioresour Technol* 97:512–521. <https://doi.org/10.1016/j.biortech.2005.02.045>
- McKay G, Blair HS, Gardner JR (1982) Adsorption of dyes on chitin. I. Equilibrium studies. *J Appl Polym Sci* 27:3043–3057. <https://doi.org/10.1002/app.1982.070270827>
- Mittal A, Mittal J, Malviya A, Gupta VK (2010) Removal and recovery of Chrysoidine Y from aqueous solutions by waste materials. *J Colloid Interface Sci* 344:497–507. <https://doi.org/10.1016/j.jcis.2010.01.007>
- Mohammad EJ, Lafta AJ, Kahdim SH (2016) Photocatalytic removal of reactive yellow 145 dye from simulated textile wastewaters over supported (Co, Ni)₃O₄/Al₂O₃ co-catalyst. *Pol J Chem Technol* 18:1–9. <https://doi.org/10.1515/pjct-2016-0041>
- Mohammadi N, Khani H, Gupta VK, Amerreh E, Agarwal S (2011) Adsorption process of methyl orange dye onto mesoporous carbon material—kinetic and thermodynamic studies. *J Colloid Interface Sci* 362:457–462. <https://doi.org/10.1016/j.jcis.2011.06.067>
- Njoku VO, Foo KY, Asif M, Hameed BH (2014) Preparation of activated carbons from rambutan (*Nephelium lappaceum*) peel by microwave-induced KOH activation for acid yellow 17 dye adsorption. *Chem Eng J* 250:198–204. <https://doi.org/10.1016/j.cej.2014.03.115>
- Pearce C (2003) The removal of colour from textile wastewater using whole bacterial cells: a review. *Dyes Pigments* 58:179–196. [https://doi.org/10.1016/S0143-7208\(03\)00064-0](https://doi.org/10.1016/S0143-7208(03)00064-0)
- Puchana-Rosero MJ, Lima EC, Ortiz-Monsalve S, Mella B, da Costa D, Poll E, Gutierrez M (2017) Fungal biomass as biosorbent for the removal of Acid Blue 161 dye in aqueous solution. *Environ Sci Pollut Res* 24:4200–4209. <https://doi.org/10.1007/s11356-016-8153-4>
- Rajendran S, Khan MM, Gracia F, Qin J, Gupta VK, Arumainathan S (2016) Ce³⁺-ion-induced visible-light photocatalytic degradation and electrochemical activity of ZnO/CeO₂ nanocomposite. *Sci Rep* 6:41. <https://doi.org/10.1038/srep31641>
- Robati D, Mirza B, Rajabi M, Moradi O, Tyagi I, Agarwal S, Gupta VK (2016) Removal of hazardous dyes-BR 12 and methyl orange using graphene oxide as an adsorbent from aqueous phase. *Chem Eng J* 284:687–697. <https://doi.org/10.1016/j.cej.2015.08.131>
- Sadaf S, Bhatti HN (2014) Batch and fixed bed column studies for the removal of Indosol Yellow BG dye by peanut husk. *J Taiwan Inst Chem Eng* 45:541–553. <https://doi.org/10.1016/j.jtice.2013.05.004>
- Saleh TA, Gupta VK (2011) Functionalization of tungsten oxide into MWCNT and its application for sunlight-induced degradation of rhodamine B. *J Colloid Interface Sci* 362:337–344. <https://doi.org/10.1016/j.jcis.2011.06.081>
- Saleh TA, Gupta VK (2012a) Photo-catalyzed degradation of hazardous dye methyl orange by use of a composite catalyst consisting of multi-walled carbon nanotubes and titanium dioxide. *J Colloid Interface Sci* 371:101–106. <https://doi.org/10.1016/j.jcis.2011.12.038>
- Saleh TA, Gupta VK (2012b) Synthesis and characterization of alumina nano-particles polyamide membrane with enhanced flux rejection performance. *Sep Purif Technol* 89:245–251. <https://doi.org/10.1016/j.seppur.2012.01.039>
- Saleh TA, Gupta VK (2014) Processing methods, characteristics and adsorption behavior of tire derived carbons: a review. *Adv Coll Interface Sci* 211:93–101. <https://doi.org/10.1016/j.cis.2014.06.006>
- Saravanan R, Gupta VK, Prakash T, Narayanan V, Stephen A (2013a) Synthesis, characterization and photocatalytic activity of novel Hg doped ZnO nanorods prepared by thermal decomposition method. *J Mol Liq* 178:88–93. <https://doi.org/10.1016/j.molliq.2012.11.012>
- Saravanan R, Joicy S, Gupta VK, Narayanan V, Stephen A (2013b) Visible light induced degradation of methylene blue using CeO₂/V₂O₅ and CeO₂/CuO catalysts. *Mater Sci Eng C* 33:4725–4731. <https://doi.org/10.1016/j.msec.2013.07.034>
- Saravanan R, Karthikeyan N, Gupta VK, Thirumal E, Thangadurai P, Narayanan V, Stephen A (2013c) ZnO/Ag nanocomposite: an efficient catalyst for degradation studies of textile effluents under visible light. *Mater Sci Eng C* 33:2235–2244. <https://doi.org/10.1016/j.msec.2013.01.046>
- Saravanan R, Karthikeyan S, Gupta VK, Sekaran G, Narayanan V, Stephen A (2013d) Enhanced photocatalytic activity of ZnO/CuO nanocomposite for the degradation of textile dye on visible light illumination. *Mater Sci Eng C* 33:91–98. <https://doi.org/10.1016/j.msec.2012.08.011>
- Saravanan R, Thirumal E, Gupta VK, Narayanan V, Stephen A (2013e) The photocatalytic activity of ZnO prepared by simple thermal decomposition method at various temperatures. *J Mol Liq* 177:394–401. <https://doi.org/10.1016/j.molliq.2012.10.018>
- Saravanan R, Khan MM, Gupta VK, Mosquera E, Gracia F, Narayanan V, Stephen A (2015a) ZnO/Ag/Mn₂O₃ nanocomposite for visible light-induced industrial textile effluent degradation, uric acid and ascorbic acid sensing and antimicrobial activity. *RSC Adv* 5:34645–34651. <https://doi.org/10.1039/C5RA02557E>
- Saravanan R, Mansoob Khan M, Gupta VK, Mosquera E, Gracia F, Narayanan V, Stephen A (2015b) ZnO/Ag/CdO nanocomposite for visible light-induced photocatalytic degradation of industrial textile effluents. *J Colloid Interface Sci* 452:126–133. <https://doi.org/10.1016/j.jcis.2015.04.035>



- Shang Y, Zhang J, Wang X, Zhang R, Xiao W, Zhang S, Han R (2016) Use of polyethyleneimine-modified wheat straw for adsorption of Congo red from solution in batch mode. *Desalin Water Treat* 57:8872–8883. <https://doi.org/10.1080/19443994.2015.1027280>
- Sivasamy A, Sundarabal N (2011) Biosorption of an azo dye by *Aspergillus niger* and *Trichoderma* sp. fungal biomasses. *Curr Microbiol* 62:351–357. <https://doi.org/10.1007/s00284-010-9713-3>
- Tan C, Li G, Lu X-Q, Chen Z (2010) Biosorption of Basic Orange using dried *A. fliculoides*. *Ecol Eng* 36:1333–1340. <https://doi.org/10.1016/j.ecoleng.2010.06.009>
- Vargas AMM, Cazetta AL, Martins AC, Moraes JCG, Garcia EE, Gauze GF, Costa WF, Almeida VC (2012) Kinetic and equilibrium studies: adsorption of food dyes Acid Yellow 6, Acid Yellow 23, and Acid Red 18 on activated carbon from flamboyant pods. *Chem Eng J* 181–182:243–250. <https://doi.org/10.1016/j.cej.2011.11.073>
- Zhang R, Zhang J, Zhang X, Dou C, Han R (2014) Adsorption of Congo red from aqueous solutions using cationic surfactant modified wheat straw in batch mode: kinetic and equilibrium study. *J Taiwan Inst Chem Eng* 45:2578–2583. <https://doi.org/10.1016/j.jtice.2014.06.009>
- Zhou T, Lu W, Liu L, Zhu H, Jiao Y, Zhang S, Han R (2015) Effective adsorption of light green anionic dye from solution by CPB modified peanut in column mode. *J Mol Liq* 211:909–914. <https://doi.org/10.1016/j.molliq.2015.08.018>

